

# Synapse Compression for Event-Based Convolutional-Neural-Network Accelerators

Lennart Bamberg, Arash Pourtaherian, Luc Waeijen, Anupam Chahar, and Orlando Moreira  
*GrAI Matter Labs* {lbamberg, apourtaherian, lwaeijen, achahar, omoreira}@graimatterlabs.ai



**Abstract**—Manufacturing-viable neuromorphic chips require novel compute architectures to achieve the massively parallel and efficient information processing the brain supports so effortlessly. The most promising architectures for that are spiking/event-based, which enables massive parallelism at low complexity. However, the large memory requirements for synaptic connectivity are a showstopper for the execution of modern convolutional neural networks (CNNs) on massively parallel, event-based architectures. This work overcomes this roadblock by contributing a lightweight hardware scheme to compress the synaptic memory requirements by several thousand times—enabling the execution of complex CNNs on a single chip of small form factor. A silicon implementation in a 12-nm technology shows that the technique increases the system's implementation cost by only below 2%, despite achieving a total memory-footprint reduction of up to  $374\times$  compared to the best previously published technique.

**Index Terms**—CNN, hardware accelerator, compression, sparsity, neuromorphic, spiking, dataflow, event based, near-memory compute

## 1 INTRODUCTION

Convolutional neural networks (CNNs) achieve state-of-the-art computer-vision performance. Neural networks are not only more accurate but also easier to develop than hand-crafted techniques. Thereby, they enable a plethora of applications, opening new markets for digital systems.

One of the main challenges CNNs pose is the combination of large computational complexity and massive parameter count (e.g., the popular *ResNet50* requires over 23M parameters and  $4\text{ GFLOPS/frame}$  [1]). Therefore, CNN inference is relatively slow and power hungry on traditional general-purpose compute architectures, as it requires a large number of expensive DRAM accesses and many arithmetic operations. This makes high frame-rate CNN inference only possible on powerful GPUs and CPUs—and not on typical edge devices. However, many computer-vision applications are located at the edge. Hence, domain-specific accelerators for efficient CNN inference are one of the largest research topics in industry and academia today.

Some of the most promising processor architectures for efficient CNN inference are dataflow/event-based with a self-contained memory organization [2]–[4]. The neuromorphic dataflow model of computation, where execution is triggered on the arrival of data exchanged through events rather than by a sequential program, enables scaling to massive core counts with low complexity. Moreover, dataflow cores are typically lighter in hardware implementation

TABLE 1

Neuron and synapse count of CNNs aside the maximum capabilities of event-based architectures from major semiconductor companies.

|                 | CNNs                 |                      |                     | Architecture   |                       |
|-----------------|----------------------|----------------------|---------------------|----------------|-----------------------|
|                 | <i>PilotNet</i> [10] | <i>MobileNet</i> [9] | <i>ResNet50</i> [1] | <i>IBM</i> [4] | <i>Intel</i> [2], [8] |
| <b>Neurons</b>  | 0.2 M                | 4.4 M                | 9.4 M               | 1.1 M          | 1.1 M                 |
| <b>Synapses</b> | 27 M                 | 0.5 B                | 3.8 B               | 0.3 B          | 0.1 B                 |

than more traditional *von-Neumann* processors. Additionally, event-based systems can exploit the large degrees of activation/firing sparsity in modern deep neural networks. This is especially true for leak-integrate-and-fire (LIF) or sigma-delta neuron models, which exploit strong temporal correlation between subsequent frames to increase sparsity [3], [5]. Thus, event-based processing delivers massive compute performance at low power consumption and area.

A self-contained memory architecture overcomes DRAM access bottlenecks, as all parameters required during execution are stored in local on-chip memories, distributed over the cores, avoiding slow and power-hungry DRAM accesses entirely. Thus, a DRAM is not required at all. Thereby, the system becomes not only more efficient but also cheaper and smaller, increasing its suitability for embedded applications.

Due to these vast promises, a range of event-based and self-contained architectures were designed by academia [6], [7], and global semiconductor companies like *Intel* and *IBM* [2]–[4], [8]. However, many of the existing chips only allow a limited neuron count and hence do not support the inference of modern sophisticated CNNs (e.g., *ResNet50* [1] or *MobileNet* [9]). The fundamental problem is the memory requirement for synapses, i.e., the (weighted) connections between the neurons. Published event-based architectures, store the synapses in (hierarchical) look-up tables (LUTs), resulting in memory requirements that scale with the total neuron count. This leads to excessive memory requirements for neural networks with a large neuron and synapse count. Consequently, architectures like *Intel's Loihi* and *IBM's TrueNorth* are not capable to execute modern, sophisticated CNNs as shown in Table 1. Sophisticated CNN models are still out of reach for existing event-based architectures, limiting their usability today.

This work overcomes this severe limitation. It contributes a technique that systematically exploits the trans-

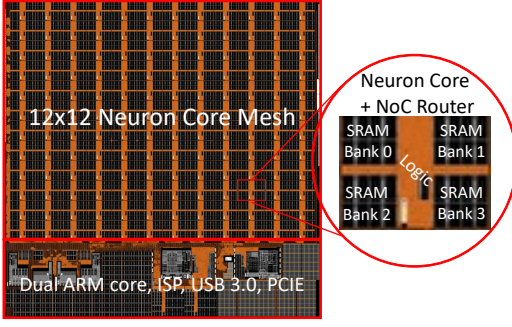


Fig. 1. Taped-out 144-neuron-core SoC with SIMD execution.

lation invariance of CNN operations to make the synaptic-memory requirements independent of the neuron count. This results in a drastic memory-footprint compression. Our technique employs two light-weight hardware blocks, a programmable event generator (PEG) and an event-to-synapse unit (ESU). Thereby, the PEG computes the synaptic connectivity of thousands of neurons—grouped in a *neuron population*—using a single instruction word, the *axon*. The ESU fills the synaptic connections with weights. Weights can be shared among all neurons of a population, reducing the memory footprint of parameters.

Our proposed technique was taped-out through the pre-commercial 144-neuron-core *GrAI-VIP* shown in Fig. 1. In the 12-nm SoC of size 60 mm<sup>2</sup>, our technique exhibits negligible implementation cost, while providing overall memory compression rates of over 300× for modern CNNs compared to the best published reference technique.

*Intel* recently revealed its new self-contained and event-based deep-neural-network (DNN) accelerator *Loihi 2*, capable to run *Nvidia's PilotNet* CNN in 30 mm<sup>2</sup> using its 4-nm technology [2]. The same network (i.e., without any optimizations) requires only 3 out of 144 cores on our chip using a 3× larger technology node at 2× the die area. This demonstrates the strong commercial value of the proposed technique, as it allows event-based cores to run much more sophisticated/complex CNNs in a temporal-sparse fashion on a single low-cost, self-contained, event-based accelerator.

The rest of this paper is structured as follows. Related work is discussed in Section 2. Section 3 includes the preliminaries covering CNNs and their sparse execution on event-based accelerators. The proposed technique is derived in Section 4. Section 5 presents experimental results. Finally, conclusions are drawn.

## 2 RELATED WORK

This section reviews related work on event-based architectures and memory-footprint compression. A wide range of massively parallel, self-contained, event-based architectures have been proposed (e.g., [2]–[4], [6]–[8]). Most only support neuromorphic neuron models, while *GrAI Matter Lab's Neuronflow* architecture [3] and the upcoming *Loihi2* [2] support also traditional DNNs—executed in a time-sparse manner to reduce the compute requirements [3], [5]. Such DNNs are today more accurate and easier to train.

Reducing the memory footprint of neural networks is an actively researched topic. Compression is vital for self-

contained architectures, as non-fitting CNNs cannot be supported. Traditional architectures have looser memory constraints due to the usage of larger DRAMs. However, even here compression has great advantages, as it reduces latency- and power-hungry DRAM accesses [11].

One approach to reduce memory requirements at system level is to use a lighter-weight CNN (e.g., [9], [12]). Another possibility is to execute a given CNN at a lower precision. A common technique is to run the network in 8-bit integer arithmetic [13], but even binary network implementations exist [14]. *Han et al.* proposed to iteratively prune weights with a small magnitude (effectively setting them to 0), followed by incremental training to recover accuracy [11]. In combination with 8-bit integer arithmetic and a weight entropy-encoding, weight pruning can achieve compression rates larger than 10× for modern CNNs [11].

The approaches mentioned so far have the advantage that they do not only reduce the memory footprint, but also the computational complexity of the CNN inference. Also, since these techniques transform the neural network itself, they are effective for most compute architectures. The drawback is that the techniques are *lossy*; i.e., they typically entail some accuracy loss, partially recoverable by retraining [11], [13].

Synapse-compression techniques for event-based systems, such as the one proposed in this work, are *orthogonal* to the *lossy* techniques discussed above. Hence, both compression types, can be applied in conjunction and studied independently. Synapse compression techniques are *lossless* and affect the implementation of the compute architecture, without changing the neural network itself. Hence, these techniques are tailored specifically for event-based systems, but entail no loss in network accuracy. Thus, they can be applied post training.

Early event-based architectures used a single routing LUT in the source to look up all synaptic connections of a neuron on its firing [6]. This approach results in many events and large memory requirements for DNNs with many neurons,  $|\mathcal{N}|$ , as the number of required bits is of complexity  $\mathcal{O}(|\mathcal{N}| \log_2(|\mathcal{N}|))$ . *Moradi et al.* and *Davies et al.*, independently, found that the events can be reduced and the synaptic-memory compressed to  $\mathcal{O}(|\mathcal{N}| \sqrt{\log_2(|\mathcal{N}|)})$  through a hierarchical, tag-based routing scheme [6], [8]. This hierarchical routing scheme found application in *Intel's* original *Loihi* architecture. The technical note of the recently released *Loihi 2* claims that the synaptic memory footprint for CNNs has been compressed again by up to 17× [2]. Unfortunately, details of the approach are (at the time of writing) not fully disclosed. However, at a reduction of “only” up to 17×, the synaptic memory requirements will still be at least of complexity  $\mathcal{O}(|\mathcal{N}|)$ . Thus, larger CNNs will remain unfeasible for *Loihi2*.

The idea of generating a synaptic memory structure for event-based CNN inference that scales independently of  $|\mathcal{N}|$  (required to run today's complex CNNs), has been tried for the *Spinnaker* chip [15]. However, the existing technique is not generic/systematic enough, as it only supports simple convolution layers. Hence, it does not support complex convolution operations with kernel stride or depth-wise operation, pooling layers, and the cutting of feature maps (FMs) in multiple fragments for compute or memory load-balancing.

Hence, the technique was only demonstrated in Ref. [15] to work for a tiny/toy CNN with five standard convolution layers and a maximum feature shape of  $28 \times 28$ . Thus, it cannot be implemented for modern deep CNNs which include more layer types, such as strided convolutions and pooling layers, as well as large FM dimensions—which make FM-cuts inevitable. Thus, the problem addressed by this work was still largely unsolved until this point.

### 3 PRELIMINARIES

#### 3.1 Neural Networks

In neural networks for image processing, a *neuron population* is represented by a three-dimensional matrix,  $\mathbf{P} \in \mathbb{R}^{D \times W \times H}$ . The last two dimensions determine the 2D Cartesian-grid position to correlate a neuron with a location in space, while the first coordinate indicates the feature (or channel) that is sampled. Thus, single neuron population represent multiple features. Here, the number of channels of such a multi-channel FM is denoted as  $D$ . The 2D submap of channel  $c_i$  ( $\mathbf{P}_{c,x,y|c=c_i}$ ) has the dimensions of a single feature, defined by a tuple: width,  $W$ , and height,  $H$ .

The raw input image represents the input population of the network. For example, a  $300 \times 300$  RGB image is represented by a  $3 \times 300 \times 300$   $\mathbf{P}$  matrix, where  $\mathbf{P}_{c,x,y}$  is the pixel value for color channel  $c$  at location  $(x, y)$ . Starting with this input population, new FMs are extracted out of the existing FMs successively (feed-forward structure). One such extraction step is symbolized as a network layer in a dataflow graph structure. The most intuitive form is a fully connected layer, in which each neuron in the destination FM,  $\mathbf{P}^+$ , is a function of all neurons in a source FM,  $\mathbf{P}$ :

$$\mathbf{P}_{c,x,y}^+ = \sigma \left( \sum_{i=0}^{D-1} \sum_{j=0}^{W-1} \sum_{k=0}^{H-1} \mathbf{W}_{c,x,y,i,j,k} \mathbf{P}_{i,j,k} + b_c \right). \quad (1)$$

Here,  $b_c$  is the bias of the neurons of feature  $c$  and  $\mathbf{W}$  is the weight matrix. DNNs can be implemented in its traditional form or as a neuromorphic/spiking leak-integrate-fire neural network (LIF-NN). In the first variant,  $\sigma()$  is a simple non-linear activation function to enable non-linear feature extraction. Typically, a rectifier/*ReLU* is used clipping all negative values to zero. The *ReLU* function exhibits low hardware complexity. Neuromorphic LIF-NNs differ from traditional DNNs through a more complex statefull activation function,  $\sigma()$ , with periodic state-leakage (details in next subsection).

A major problem with fully connected layers is the large number of synaptic weights determining the compute and memory requirements. For example, an extraction of ten  $300 \times 300$  features from a  $3 \times 300 \times 300$  FM requires 243 M weights and multiply-accumulate (MAC) operations. This can be overcome by exploiting *spatial locality* [16]. For a meaningful feature extraction, its not needed to look far in XY to glean relevant information for one XY coordinate of the extracted feature. Thus, outside a relative range of XY size ( $KW, KH$ )—denoted as convolution kernel—all synapses/connections between neurons are removed. This drastically reduces the compute and memory requirements in so-called locally connected 2D layers.

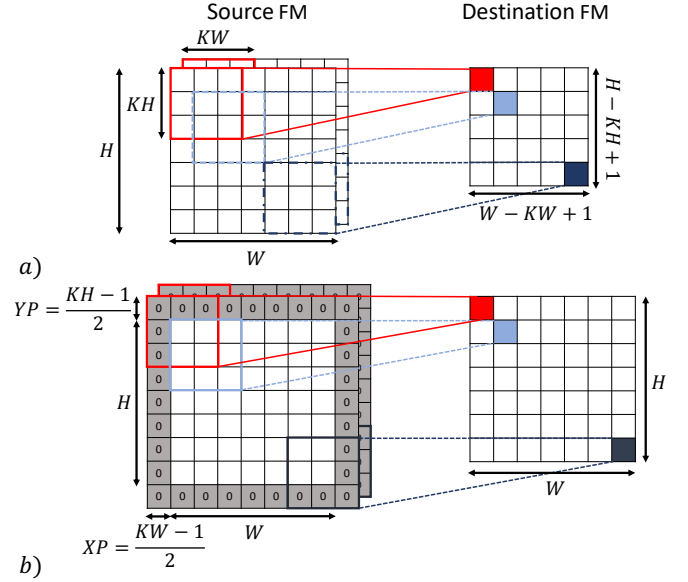


Fig. 2. Convolution operation without padding (a), and with *same* zero-padding (b) resulting in no resolution reduction.

Moreover, network filters should respond similarly to the same patch, irrespective of its XY location in the source FM. This principle is called *translation invariance* [16]. Hence, the relative weights can be independent of the XY location of the destination neuron, i.e., weights can be reused for all neurons of the same channel. This further reduces the memory requirements.

The regular convolution operation in a CNN adds both, spatial locality and translation invariance (compared to fully connected layers). This results in the following formula for a convolution layer with a kernelsize of  $KW \times KH$ :

$$\mathbf{P}_{c,x,y}^+ = \sigma \left( \sum_{i=0}^{D-1} \sum_{j=0}^{KW-1} \sum_{k=0}^{KH-1} \mathbf{W}_{c,i,j,k} \mathbf{P}_{i,x+j,y+k} + b_c \right). \quad (2)$$

The XY size of the extracted FM in a convolution operation is the XY size of the source FM minus  $KW - 1$  in width and  $KH - 1$  in height. This is how often the convolution kernel fits in the source FM, illustrated in Fig. 2.a. Padding rows and columns of zeros around the source can be done to control the size of the output FM. To achieve an output of the same size as the input (i.e., to preserve the feature resolution), one must pad  $(KH-1)/2$  rows of zeros at the top and bottom of the source FM, and  $(KW-1)/2$  columns at the left and right. This zero-padding is illustrated in Fig. 2.b.

Instead of padding the source FM in a pre-processing step, the effect of zero padding can also be expressed implicitly, by changing the source-FM indices in Eq. (2):

$$\mathbf{P}_{c,x,y}^+ = \sigma \left( \sum_{i=0}^{D-1} \sum_{j=0}^{KW-1} \sum_{k=0}^{KH-1} \mathbf{W}_{c,i,j,k} \mathbf{P}_{i,x+j-XP,y+k-YP} + b_c \right) \quad \text{with } \mathbf{P}_{i,x,y} = 0 \text{ for } x < 0 \text{ or } y < 0. \quad (3)$$

Here,  $XP$  and  $YP$  are the rows/columns of zeros padded at the left and the top of the source FM, respectively.

Kernel striding and source upsampling are other ways of controlling the dimensions of the extracted features. With a stride of two, the kernel is not shifted by one step for every generated output point but by two, resulting in extracted features with a 50 % smaller resolution. When the source is upsampled to increase the resolution of the extracted features, zeros are filled between the upsampled source values followed by a trainable convolution on the upsampled map.

### 3.2 Event-Based Architectures

In this section, we outline the conceptual idea of event-based compute architectures for efficient CNN inference. These architectures exhibit massive parallelism with many identical cores connected through a network-on-chip (NoC), enabling scaling to thousands of cores [2], [6].

To each of the  $C$  cores, one or more neuron populations,  $\mathbf{P}_i$ , are statically mapped. Near-memory computing is applied in the architectures. Thus, the entire memory is distributed equally over the cores, and the neural parameters (i.e., weighted synapses) are stored in the cores their respective neurons are mapped to. The dynamic variables, computed by one core (i.e., the activated neuron states; see Eq. (3)) and required by other cores for the accumulation of their assigned neuron states, are explicitly exchanged in the form of events over the NoC. Hence, there are no coherence problems. This allows the removal of higher (shared) memory levels, improving latency and power consumption. However, since the on-chip memories of the cores have a limited capacity, the static/compile-time mapping of neuron populations to cores must satisfy hard memory constraints; i.e., the number of neurons and synapses that can fit in a core is limited by the core's memory capacity. If a neuron population  $\mathbf{P}_i$  representing an FM of the CNN includes too many parameters or neurons, it needs to be split/cut into two or more smaller populations  $\mathbf{P}_i^{(1)}$  and  $\mathbf{P}_i^{(2)}$  before core assignment.

Computation in a core is triggered by the arrival of data in form of events (dataflow execution). Received events are stored in an event buffer for FIFO processing to reduce backpressure effects. When an event is processed, its value is multiplied with the weights of the synapses between the source neuron and the destination neurons mapped to the core. The results are accumulated to the destination neuron states. After their computation, activated neuron states are sent through events to all connected neurons in the following layers. Since these neurons can be mapped to any core in the cluster, events can also be injected into the local event queue instead of going out on the NoC.

Note that above we describe how more recent architectures (considered in this paper) work. In some earlier architectures, the multiplication of activations and synaptic weights are executed at the source (before event transmission), and event processing at the destination only requires the addition of the event value to the target neuron state [6]. This results in more events being generated for neurons with multiple synapses and affects the synaptic memory structure described later.

#### 3.2.1 Sparsity Exploitation in Event-based Architectures

During DNN execution, no events are generated for zero-valued activations. Skipping zero-valued events induces no

neuron-state accumulation error due to the linearity of MAC operations. Thus, each zero in an FM reduces the compute and communication requirements of an inference—saving energy and compute resources. This is a tremendous advantage of event-based architectures compared to more traditional architectures. Particularly for modern CNNs with large degrees of activation sparsity (i.e., zero-valued activations), this gives event-based architectures a clear power-performance advantage. Standard CNNs exhibit an activation sparsity of about 50 % when a *ReLU* activation function is used, as it clips all negative neuron potentials to zero. Thus, event-based processing improves the power-delay product by about  $4\times$ , without any accuracy loss.

Event-based architectures can offer even larger gains by implementing CNNs as LIF-NNs or sigma-delta neural networks (SD-NNs) to increase sparsity. A LIF-based CNN has the same synaptic connectivity as the respective standard CNN implementation [17]. However, LIF-NNs exhibit a more complicated firing behavior—expressed by  $\sigma()$  in Eq. (3)—that increases sparsity but also makes back-propagation training hard. Consequently, LIF-NNs cannot compete with standard CNNs accuracy-wise for complex vision applications. To address this, SD-NN implementations increase the activation sparsity by turning the strong temporal correlation of neuron potentials between subsequent frames of a time-continuous stream (e.g., video) into event sparsity [5]. By keeping memory for a persistent accumulator state for each neuron, the temporal deltas in the activations can be exchanged/processed (instead of absolute values). Still, the exact same inference results as the standard CNN implementation are obtained as state accumulation is a linear operation. Hence, SD-NNs have no training or accuracy issues, as they can use any standard CNN and provide the same accuracy without retraining. Nevertheless, they heavily improve sparsity, as the temporal deltas of the activations exhibit even more zeros than the absolute activation maps, due to the strong temporal correlation—especially if activations are quantized [5]. Thereby, SD-NNs increase the gains of event-based processing even further without scarifying any accuracy.

Since the proposed, as well as the reference techniques, work for all three described DNN implementations (standard, LIF, and SD), from this point onwards, we use the term *firing neuron* in this work to describe a neuron of any type for which the synaptic connectivity has to be activated due to a non-zero activation, activation-delta, or spike.

#### 3.2.2 Synaptic-memory in Existing Architectures

Event-based accelerators need information on the synaptic connectivity of a firing neuron to know which neurons to update with which weights. Mathematically, the connectivity of neurons can be described as a directed graph  $\mathcal{G} = (\mathcal{N}, \mathcal{S})$ , where  $\mathcal{N}$  and  $\mathcal{S}$  are the sets of neurons and synapses, respectively. Each synapse,  $s_i \in \mathcal{S}$ , can be described by a tuple  $(n_{\text{src}}, n_{\text{dst}}, w)$ , where  $(n_{\text{src}}, n_{\text{dst}}) \in \mathcal{N}^2$  is the synapse's source and destination neuron, respectively, and  $w$  is the synaptic weight.

In early event-based accelerators, the synapse information is simply stored in LUTs, mapped to the cores together with the neurons. On the firing of a neuron, the addresses of the destination neurons together with the



weights/parameters are looked-up, and for each pair an event carrying the firing value times the weight is emitted towards the destination neuron. Considering an average number of  $F$  outgoing synapses per neuron, the required memory bits to store the connectivity (i.e., synapses without the weights) for  $|\mathcal{N}|$  neurons in this scheme is

$$Mem_c = |\mathcal{N}|F \log_2(|\mathcal{N}|). \quad (4)$$

For  $B$ -bit weights, the parameter requirements become

$$Mem_p = |\mathcal{N}|FB. \quad (5)$$

For densely connected networks with many neurons, a LUT results in huge memory requirements. As an illustrative example, let us investigate the last  $3 \times 3$  convolution of the *ResNet50* CNN [1], with  $512 \times 7 \times 7$  ( $=25$  k) neurons in the source and destination. The memory requirements of this single layer for 8-bit weights and the connectivity is at least 201 MB and 110 MB, respectively.

Moreover, the standard LUT-based approach has the disadvantage that it results in one event per synapse (so  $F$  events per firing neuron). The number of events and the memory requirements can be reduced through a hierarchical/two-stage LUT layout [6], [8]. For each spiking neuron, only the addresses of the destination cores are looked up in the first routing table at the source. Thus, only one event is generated per destination core instead of one per destination neuron (while hundreds of neurons can be mapped to one core). The events contain a  $K$ -bit tag (stored in the LUT at the source) and the firing value. In the destination core, the weights and the target neurons are selected based on the tag through a second LUT.

Assuming a maximum fan-in (i.e., number of in-going synapses) per neuron of  $F_{\max}$ , the tag-width has to be at least  $\log_2(F_{\max})$  to make the approach work. With  $C$  cores,  $M$  neurons per core, and a neuron fan-in

of  $F$ , the number of bits to store the connectivity of  $|\mathcal{N}|$  neurons reduces to

$$\begin{aligned} Mem_c &= Mem_{c,src} + Mem_{c,dst} \\ &= |\mathcal{N}| \left( \frac{F}{M} \log_2(F_{\max} C) + \log_2(F_{\max}) F \right), \end{aligned} \quad (6)$$

in the best case. However, the memory requirement still scales with  $|\mathcal{N}|$ , making the scheme impractical for modern CNNs. Analyzing again the last  $3 \times 3$  convolution of *ResNet50*, the memory requirement for connectivity is still at least 167 MB.

For the sake of fairness, we want to clarify that the considered reference architectures were designed to support all kinds of neural networks, not only CNNs. However, each of them show-cased CNNs as one of the most relevant application scenarios. For neural networks that are more sparsely connected and have fewer neurons than modern CNNs, existing schemes will work without severe memory issues. However, for modern deep CNNs, existing techniques must be extended by a scheme in which the synaptic memory requirement is entirely independent of the neuron count  $|\mathcal{N}|$  to enable their execution on event-based architectures with a reasonable memory capacity.

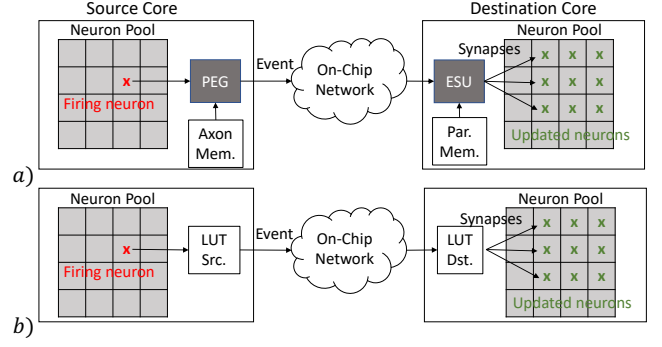


Fig. 3. a) Proposed technique based on two hardware blocks. b) Reference technique based on a hierarchical LUT.

## 4 TECHNIQUE

In the following, we propose a technique to compress the synapses for CNNs such that the memory requirements no longer scale with the neuron count but just with the population count. Fig. 3 illustrates the idea compared to the existing hierarchical-LUT scheme. We propose to use two hardware blocks, a programmable event generator (PEG) and an event-to-synapse unit (ESU) rather than LUTs.

To avoid memory requirements per neuron, so-called *axons* in the source connect entire neuron populations instead of individual neurons. For each population,  $P_{dst,i}$ , with at least one synapse directing from the current population,  $P_{src,i}$ , an axon is stored at the source. Axons can be seen as the PEG's instructions, defining simple routines executed on the firing of any neuron to generate the required events. Besides the *axon(s)* of the population, the PEG needs information on the firing neuron. Like the reference technique, our technique results in low NoC bandwidth requirements, as the PEG generates at most one event per axon.

The ESU in the destination core decodes the event into weighted synapses. The ESU uses weight sharing between different synapses. This means that events that originate from the same FM, but from different neurons, can use the exact same weights without having to store them multiple times. This yields high weight-compression rates on top of the savings provided by the axon scheme, due to the translation invariance of CNN operations.

In the following subsections, we successively derive the architecture of the PEG and ESU to support state-of-the-art CNNs at a maximized compression rate. We start by looking at the simple case of a regular convolution. First, we assume that the compute and memory capacity of each core is large enough that it is not needed to split any multi-channel FM into several populations mapped onto different cores. In the next subsections, we will extend the approach to cover FM fragmentation and other layer types found in today's CNNs.

### 4.1 Basic Technique

To identify which outgoing synapses a firing neuron has, we have to view the convolution operation in a transposed, i.e. event-based, manner. While the traditional view (illustrated in Fig. 4.a for a single channel) reduces source values via the kernel, the event-based one broadcasts source elements

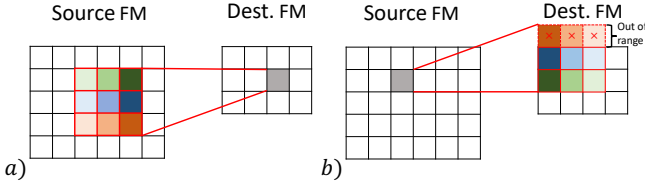


Fig. 4. Regular (a) and event-based (b) implementation of a convolution.

**Algorithm 1** PEG for a regular convolution.

---

**Require:** Firing neuron & value:  $x_{src}, y_{src}, c_{src}, v$   
**Require:** Axon set of population:  $\mathcal{A}$

- 1: **for**  $A = (X_{off}, Y_{off}, AD_c, ID_p) \in \mathcal{A}$  **do**
- 2:    $x_{min}, y_{min} = (x_{src}, y_{src}) + (X_{off}, Y_{off})$
- 3:    $gen\_event(AD_c, ID_p, x_{min}, y_{min}, c_{src})$
- 4: **end for**

---

via the transposed kernel (illustrated in Fig. 4.b). Event processing adds the event value multiplied with the respective weight to any neuron state/accumulator in the range of the transposed kernel. The final neuron states for the inference are obtained after all events have been processed.

To obtain the exact same final neuron states in the event-based implementation as in the standard implementation, the weight arrangement in the broadcasted kernel must be transposed in XY (e.g., top-left weight becomes bottom-right). In the common view, the reduced destination neuron's XY coordinate is the upper-left anchor point of the kernel in the source-FM. In the event-based variant, the XY location of the broadcasted source neuron is the bottom-right anchor point of the transposed kernel in the destination FM. The convolution formula with implicit padding (Eq. (3) on page 3) reveals that padding shifts the XY coordinate of the bottom-right anchor-point of the transposed kernel by the padding amount,  $(XP, YP)$ .

Thus, on the firing of a neuron on channel  $c_{src}$  with XY coordinate  $(x_{src}, y_{src})$ , all neurons (of any channel) in the destination FM must be updated whose X and Y coordinate is in  $(x_{src} - KW + XP, x_{src} + XP]$  and  $(y_{src} - KH + YP, y_{src} + YP]$ , respectively. In that range, the XY-transposed kernel weights  $\mathbf{W}_{i,j,k,l}|_{l=c_{src}}$  are scaled (i.e., multiplied) with the firing value and added to the respective neuron states. For some firing neurons nearby the edges of an FM, part of the broadcasted kernel does not overlap with the destination FM, as illustrated in Fig. 4.b. Such kernel parts located outside the FM boundaries do not result in neuron updates and thus are skipped in the ESU.

The pseudo codes in Alg. 1 and Alg. 2 describe the required functionality of the PEG and the ESU, respectively, implemented in hardware through simple state machines. The PEG of the source core (i.e., the core with the firing neuron) calculates the top-left anchor point for the transposed convolution kernel in the destination FM,  $(x_{min}, y_{min})$ . As we have shown before, this requires a subtraction of  $(KW - XP - 1, KH - YP - 1)$  from the XY coordinate of the firing neuron  $(x_{src}, y_{src})$ . Since the padding and kernel shape are constant at run-time, this is done in the PEG at once by adding a signed offset pair to the neuron's coordinates:

$$X_{off}, Y_{off} = (-KW + XP + 1, -KH + YP + 1) \quad (7)$$

**Algorithm 2** ESU for a regular convolution.

---

**Require:** Event body:  $x_{min}, y_{min}, c_{src}, v$   
**Require:** Neuron population & shape:  $\mathbf{P}, D, W, H$   
**Require:** Transposed weights & kernel size:  $\mathbf{W}, KW, KH$

- 1: **for**  $\Delta x \in [0, KW)$  **do**
- 2:    $x = x_{min} + \Delta x$
- 3:   **continue if**  $x \notin [0, W)$  // kernel part out of range?
- 4:   **for**  $\Delta y \in [0, KH)$  **do**
- 5:      $y = y_{min} + \Delta y$
- 6:     **continue if**  $y \notin [0, H)$  // kernel part out of range?
- 7:     **for**  $c \in [0, D)$  **do**
- 8:       // update\_neuron depends on neuron model
- 9:        $update\_neuron(\mathbf{P}_{c,x,y}, \mathbf{W}_{c,\Delta x,\Delta y,c_{src}}, v)$
- 10:     **end for**
- 11:   **end for**
- 12: **end for**

---

Pre-calculating the offset values at compile time, stored in the axon rather than the kernel shape and the padding, saves additions/subtractions in the PEG for each firing neuron at run-time, as well as bits in the axon.

The outgoing event generated by the PEG contains the computed  $(x_{min}, y_{min})$  coordinates, which can contain negative values if the top-left anchor-point is located outside the FM range. Moreover the firing value,  $v$ , and the channel of the firing neuron,  $c_{src}$ , are added to the event body. At last, events need the NoC address of the core to which the target population is mapped,  $AD_c$ , as well as a destination-population identifier,  $ID_p$ , such that multiple populations can be mapped onto cores. These last two parameters are static and are thus directly stored in the axon.

Each source population has an independent axon for each directly connected destination population. On each firing, the PEG must process all axons to generate events towards all populations.

At the far end, the ESU takes the event and selects the needed transposed 3D kernel,  $\mathbf{W}_{i,j,k,l}|_{l=c_{src}}$  based on  $c_{src}$  and  $ID_p$  from the event. It applies the weights scaled with the event value on the neurons with the top-left anchor-point taken from the event  $(x_{min}, y_{min})$ . It skips kernel parts that do not overlap with the population. The iteration order is depth/channel-first. This minimizes the amount of required *continue* statements to at most  $KH \cdot KW$ , reducing the complexity for the hardware implementation.

The proposed technique shares kernels and axons among all neurons of a population. Therefore, besides axons, neurons, and weights, we need two more types of memory words: population descriptors and kernel descriptors. The population descriptor contains the 3D neuron population shape, the neuron type, the start address of the state values, and the number of axons linked to the population. A kernel descriptor contains the kernel shape, its weight width, and the starting memory-address of the weights.

**4.2 Support for FM Cutting**

A multi-channel FM in the original/pre-mapped CNN graph can have so many parameters or neurons that it cannot be mapped onto a single core due to memory or compute constraints. In this case, our technique allows to cut FMs into several smaller neuron populations, mapped onto different cores.

An FM cut that splits the channels results in a reduction in the number of neurons as well as weights that have to be

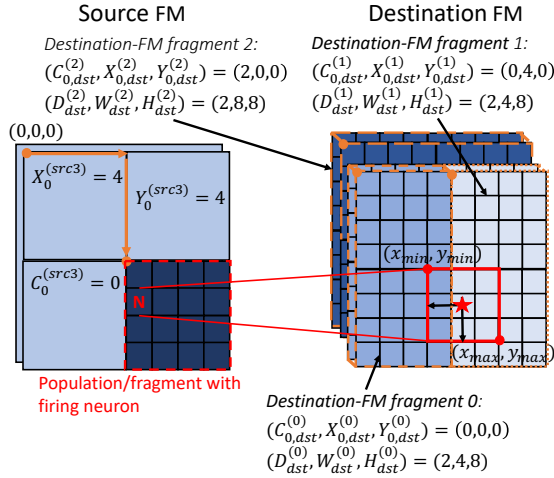


Fig. 5. Cutting of the source and the destination FM.

mapped per core. On the other hand, a cut in the XY space of the features requires all populations to contain all kernel weights, due to the translation invariance of the convolution operation. Hence, a cut reducing only the X and/or Y size of the individual populations increases the memory requirements noticeably, as shared weights are duplicated (i.e., mapped onto multiple cores). Nevertheless, our approach supports both: cuts in channel-coordinate  $C$  and XY. The rationale is that, for high-resolution features, it may happen that even a single channel does not fit into a core, making XY cuts inevitable. Also, addressing limitations can result in inevitable XY cuts. For example, for 8-bit population-width/height fields, a high-resolution FM has to be split into populations with a width and height of at most 255.<sup>1</sup>

Fig. 5 shows an example where the source and destination FM are cut into four and three pieces, respectively. The example helps to understand the following mathematical derivation of the FM-fragmentation technique.

Let the shape of the original, unfragmented  $i^{\text{th}}$  FM be  $(D_{\text{pre},i}, W_{\text{pre},i}, H_{\text{pre},i})$ . The FM is cut into  $M$  disjunct populations  $\mathbf{P}_i^{(0)}, \mathbf{P}_i^{(1)}, \dots, \mathbf{P}_i^{(M-1)}$ . The shape of the  $j^{\text{th}}$  fragment is  $(D_i^{(j)}, W_i^{(j)}, H_i^{(j)})$  and it contains all neurons from the original FM with  $c \in [C_{0,i}^{(j)}, C_{0,i}^{(j)} + D_i^{(j)}]$ ,  $x \in [X_{0,i}^{(j)}, X_{0,i}^{(j)} + W_i^{(j)}]$ , and  $y \in [Y_{0,i}^{(j)}, Y_{0,i}^{(j)} + H_i^{(j)}]$ . Thus,  $(C_{0,i}, X_{0,i}, Y_{0,i})$  is the coordinate of the first, upper-left neuron of the fragment. For a valid fragmentation, each neuron must be mapped to exactly one population. This is satisfied if the neuron populations after fragmentation are disjoint and if the number of neurons in the pre-mapped FM is the same as the sum of the number of neurons of the individual fragments.

Next, we discuss how to adapt the PEG to cope with FM cuts. When a neuron fires in a possibly cut population, its coordinates  $(c_{\text{src}}, x_{\text{src}}, y_{\text{src}})$  are the ones relative to the start of the neuron-population/fragment, not the entire FM. Adding to the neuron's coordinates the start point of the fragment (presented by the population) in the original FM,  $(C_{0,\text{src}}, X_{0,\text{src}}, Y_{0,\text{src}})$ , results in the neuron's coordinates in the original/uncut FM. Thus, the upper-left anchor point of

the broadcasted kernel in the original destination FM and the channel of the firing neuron are calculated as

$$\begin{aligned} c_{\text{src,orig}} &= c_{\text{src}} + C_{0,\text{src}} \\ x_{\text{min,orig}} &= x_{\text{src}} + X_{0,\text{src}} - KW + XP + 1 \\ y_{\text{min,orig}} &= y_{\text{src}} + Y_{0,\text{src}} - KH + YP + 1. \end{aligned} \quad (8)$$

For each fragment of the destination FM, we can then calculate the upper-left anchor point of the transposed kernel relative to their XY start-point in the original FM:

$$\begin{aligned} x_{\text{min}} &= x_{\text{min,orig}} - X_{0,\text{dst}} \\ &= x_{\text{src}} + X_{0,\text{src}} - KW + XP + 1 - X_{0,\text{dst}} \\ y_{\text{min}} &= y_{\text{min,orig}} - Y_{0,\text{dst}} \\ &= y_{\text{src}} + Y_{0,\text{src}} - KH + YP + 1 - Y_{0,\text{dst}}. \end{aligned} \quad (9)$$

These  $(x_{\text{min}}, y_{\text{min}})$  coordinates, together with  $c_{\text{src,orig}}$ , must be sent via an event to the core of the destination-FM fragment.

All parameters but the coordinates of the firing neuron in Eq. (9) are static at run-time. Thus, supporting FM cuts just needs an adjustment of the X and Y offset values calculated at compile time, plus an additional offset value for the channel coordinate:

$$\begin{aligned} C_{\text{off}} &= C_{0,\text{src}} \\ X_{\text{off}} &= X_{0,\text{src}} - KW + XP + 1 - X_{0,\text{dst}} \\ Y_{\text{off}} &= Y_{0,\text{src}} - KH + YP + 1 - Y_{0,\text{dst}}. \end{aligned} \quad (10)$$

Note that the offset values for X and Y can now be negative. Thus, they have to be stored as signed values. The channel offset is always positive. Hence, it is an unsigned value.

An axon is needed for each fragment of the source FM, per fragment of the destination FM, as each pair needs different offset values. However, the number of events and axons is still minimal, as different populations are mapped onto different cores. Thus, different axons and events are required in any case, due to the varying core addresses.

Each core only stores the weights for the channels that are mapped to it. Thus, the indexes of the weight matrix are relative to the first channel of the respective fragment; i.e., when neurons of the channels 4–8 are mapped onto a core,  $\mathbf{W}_{0,0,0,0}$  in the core is the upper-left kernel weight for source channel 0 and destination channel 4 from the original weight matrix. This segmentation of the weight matrix is done entirely at compile time.<sup>2</sup>

In summary, besides an additional axon parameter  $C_{\text{off}}$  added to the channel coordinate, nothing must be changed in the PEG hardware. The ESU must not be modified at all. However, there is another optimization we can add to the PEG, which is a *hit detection* to filter out unnecessary events which an ESU decodes in 0 synapses.

Consider in Fig. 5, that the neuron at position (0,1,1)—not the one highlighted at position (0,0,1)—of the source-FM fires. The PEG depicted by Alg. 1 sends an event to the core destination-FM fragment 0 is mapped onto. This event has an  $x_{\text{min}}$  value of 4. However, the population only contains neurons with  $x \in [0, 3]$ . Thus, decoding the event in the ESU at the receiving side results in no activated synapse, as no part of the kernel overlaps with the population (i.e., for loop in line 1 of Alg. 2 has an empty range). The system functions

1. Such fragments can be mapped to the same core to share weights.

2. The weight segmentation is only disjunct for no X or Y cuts.



**Algorithm 3** PEG for a regular convolution with support for FM fragmentation and empty-event skipping.

---

**Require:** Firing neuron & value:  $x_{src}, y_{src}, c_{src}, v$   
**Require:** Axon set of population:  $\mathcal{A}$

```

1: // grayed hit-detection only needed with many XY cuts
2: for  $(X_{off}, Y_{off}, C_{off}, W, H, KW, KH, AD_c, ID_p) \in \mathcal{A}$  do
3:    $x_{min}, y_{min}, c_{src} = (x_{src}, y_{src}, c_{src}) + (X_{off}, Y_{off}, C_{off})$ 
4:    $x_{max}, y_{max} = (x_{min}, y_{min}) + (KW, KH)$ 
5:   if  $(x_{min} < W) \& (x_{max} > 0) \& (y_{min} < H) \& (y_{max} > 0)$  then
6:      $gen\_event(AD_c, ID_p, x_{min}, y_{min}, c_{src})$ 
7:   end if
8: end for

```

---

correctly, but the transmitted and decoded events yielding no activated synapses waste energy and computation. Such events could be filtered out by the PEG.

This PEG power-performance optimization is achieved by calculating not only the minimum X and Y coordinates of the neurons in the kernel range (i.e., the relative top-left coordinate of the projected kernel), but also the first X and Y coordinates outside the range. These coordinates are  $(x_{min}, y_{min}) + (KW, KH)$ . We can then check if the kernel overlaps with at least one neuron of the population by means of simple Boolean operations. If it does not, no event is generated. For this, axons must contain the kernel shape as well as the width and height of the target population.

A hit-detection in the channel coordinate is not required, as all channels in the XY kernel range are updated at the destination, irrespective of the channel of the firing neuron. Thus, if cutting in XY is the rare exception—plausible due to the implied unwanted weight-duplication of such cuts—hit detection can be skipped to reduce the PEG hardware cost. However, we propose to add hit-detection as it has reasonable hardware costs, while embedded architectures typically aim at low bit widths for encoding, resulting in more XY fragmentation for high-resolution FMs. Alg. 3 shows the pseudo code for the PEG with support for FM fragmentation and hit detection.

### 4.3 Down- and Upsampling Support

In the following, we extend the PEG-ESU pair to support upsampling and strided convolutions. A kernel stride of  $N$  in a convolution results in the same extracted FM as applying the convolution kernel regularly (i.e., with a stride of 1) followed by a downsampling of the resulting FM by factor  $N$  in X and Y. Keeping that in mind, we derive a way to support strided convolutions by adjusting the ESU.

The pseudo code of the ESU with support for programmable kernel striding is shown in Alg. 4. We add a field  $SL$ , containing the  $\log_2$  of the applied kernel stride, to the kernel descriptor. Through  $SL$ , the ESU knows which rows and columns to skip as they are gone after down-sampling. The PEG still behaves as it would for regular convolutions. Hence,  $W$  and  $H$  of the axon for the width and height of the destination fragments (in case hit-detection is implemented) are the ones that would be obtained for a stride of 1; i.e. the true physical width,  $W_t$ , and height,  $H_t$ , after down-sampling shifted left by  $SL$  ( $W_t \ll SL$  and  $H_t \ll SL$ ). Also the offset values must be adjusted to equalize the

**Algorithm 4** ESU with support for strided convolutions.

---

**Require:** Event body:  $x_{min}, y_{min}, c_{src}, v$   
**Require:** Neuron population & descriptor:  $\mathbf{P}, D, W, H$   
**Require:** Trans. weights & descriptor:  $\mathbf{W}, KW, KH, SL$

```

1: for  $\Delta x \in [0, KW)$  do
2:    $x = x_{min} + \Delta x$ 
3:   continue if  $x \notin [0, W)$  or  $x \pmod{2^{SL}} \neq 0$ 
4:   for  $\Delta y \in [0, KH)$  do
5:      $y = y_{min} + \Delta y$ 
6:     continue if  $y \notin [0, H)$  or  $y \pmod{2^{SL}} \neq 0$ 
7:      $x, y = (x, y) \gg SL$  // XY down-sampling
8:     for  $c \in [0, D)$  do
9:        $update\_neuron(\mathbf{P}_{c,x,y}, \mathbf{W}_{c,\Delta x,\Delta y,c_{src}}, v)$ 
10:    end for
11:  end for
12: end for

```

---

downsampling of the destination FM:

$$\begin{aligned} X_{off} &= X_{0,src} - KW + XP + 1 - (X_{0,dst} \ll SL) \\ Y_{off} &= Y_{0,src} - KH + YP + 1 - (Y_{0,dst} \ll SL). \end{aligned} \quad (11)$$

All this only affects parameters stored at compile-time in the axons. Thus, the PEG hardware remains unchanged.

Also, the ESU initially behaves as for a regular convolution. Thus, also here the true population width and height shifted left by  $SL$  are stored in the descriptor as  $W$  and  $H$ , respectively. The effective downsampling after convolution due to the kernel stride is considered by extending the *continue* conditions. In detail, if the *for-loop* iteration over the transposed kernel is at a row or column removed by the downsampling, synapse generation for that part of kernel is skipped. Rows and columns that are not skipped are only the ones with  $X$  or  $Y$  coordinates which are modulo  $2^{SL}$  equal to 0. For non-skipped kernel parts, the downsampling of the XY coordinate is applied for the selection of the neuron to be updated. This down-sampling is realized in hardware at a low cost through a right shift by  $SL$ .

At a first glance, it might seem that adding stride support adds noticeably to the complexity of the ESU. However, this is not the case. First, checking that a binary signal is not 0 in modulo  $2^{SL}$  just requires to logically OR the last  $SL$  bits. Moreover, for all common CNNs, at most a kernel stride of 2 is used at a given layer. Thus, we propose to keep  $SL$  a 1-bit value such that a stride of 1 (regular convolution) or 2 can be applied in a single step. Larger strides can still be implemented in that case by inserting dummy/identity layers with another stride of two until the needed downsampling is reached. This follows the architectural principle of optimizing for the common case, with non-optimized support for the uncommon case. With a 1-bit  $SL$  field, checking that a signal is not 0 modulo  $2^{SL}$ , requires only a single AND-gate with  $SL$  and the signal's LSB as the Boolean inputs. Moreover, with a 1-bit  $SL$  value, also shifting left by  $SL$  has ultra-low cost. It can be synthesized in a single 2-to-1 multiplexer with  $SL$  as the select signal. Thus, the hardware costs for adding stride support are low.

Next, we discuss the PEG changes to support upsampling the source, required for example for fractionally-strided convolution [18]. Thereby, zeros are filled between the upsampled source values. After upsampling, a convolution operations is applied. To implement source upsampling through the PEG, the XY coordinates of the firing neuron must be shifted left by the  $\log_2$  of the upsampling factor,



**Algorithm 5** PEG with upsampling support.

---

**Require:** Firing neuron & value:  $x_{src}, y_{src}, c_{src}, v$   
**Require:** Axon set of population:  $\mathcal{A}$

```

1: // grayed hit-detection only needed with many XY cuts
2: for  $(X_{off}, Y_{off}, C_{off}, W, H, KW, KH, US, AD_c, ID_p) \in \mathcal{A}$  do
3:    $x_{src}, y_{src} = (x_{src}, y_{src}) \ll US$  // XY up-sampling
4:    $x_{min}, y_{min}, c_{src} = (x_{src}, y_{src}, c_{src}) + (X_{off}, Y_{off}, C_{off})$ 
5:    $x_{max}, y_{max} = (x_{min}, y_{min}) + (KW + KH)$ 
6:   if  $(x_{min} < W) \& (x_{max} > 0) \& (y_{min} < H) \& (y_{max} > 0)$  then
7:      $gen\_event(AD_c, ID_p, x_{min}, y_{min}, c_{src})$ 
8:   end if
9: end for

```

---

$US$ , before adding the offset value. Also, the formulas for the X and Y offset values calculated offline must consider the upsampling on the source values  $X_{0,src}$  and  $Y_{0,src}$ :

$$\begin{aligned} X_{off} &= (X_{0,src} \ll US) - KW + XP + 1 - (X_{0,dst} \ll SL) \\ Y_{off} &= (Y_{0,src} \ll US) - KH + YP + 1 - (Y_{0,dst} \ll SL). \end{aligned} \quad (12)$$

The resulting final pseudo code of the PEG with stride support is shown in Alg. 5.

#### 4.4 Other Layer-Types

Today's CNNs contain various layer types. The proposed PEG-ESU pair supports (most of) them without further hardware changes, as shown in the following for the most relevant examples.

**Deconvolutions (Transposed Convolutions):** Deconvolutions are used to inverse convolution operations. They are typically implemented as a transposed convolution operation shown in Fig. 4.b with the addition that the source padding and destination FM size is adjusted such that the transposed kernel always fully overlaps with the destination FM. Thus, transposed convolutions are naturally supported by the proposed technique.

**Concatenation & Split Layers:** Some neural networks have multiple branches that are at some point concatenated into one. This concatenation and splitting can be implemented by the PEG without further ado due to the support of FM fragmentation, described in Subsection 4.2.

**Dilated Convolutions:** Dilated convolutions increase the receptive field of the kernel without increasing the number of trainable parameters by having holes between the trainable weights of the kernel. The X or Y hole between two weights is called the *dilation rate*. Hardware support for efficient dilated convolutions can be easily added. However, dilated convolutions are not found in most of today's CNNs. Hence—based on the architectural principle to only optimize for the common case—we propose to implement dilated convolutions, simply as regular convolutions. If  $DR$  is the dilation rate, the used regular convolution kernel has an XY shape of  $(DR \cdot KW - DR + 1) \times (DR \cdot KH - DR + 1)$ , where zeros are filled at the intermediate position. Ideally, this is paired with an efficient zero-weight skipping technique as it is done in our *GrAI-VIP* architecture, enabling an additional drastic weight compression through pruning [11].

**Depthwise & Grouped Convolutions:** A depthwise convolution is a lightweight filtering, applying a single convolution per input channel (i.e., no channel mixing;  $i^{\text{th}}$

output channel only depends on  $i^{\text{th}}$  input channel instead of all). In a grouped convolution, each output channel depends on a small set of input channels,  $D_{\text{group}}$ . Depthwise and grouped convolutions can be implemented with the ESU-PEG pair by (virtually) splitting the original source and destination FM into many FMs of depth 1 (depthwise) or  $D_{\text{group}}$  (grouped), with regular convolution operations between the source-destination pairs covering the same channel(s).

**Average & Max. Pooling:** Pooling operations are implemented as strided depthwise convolutions. For example, an average pooling over non-overlapping  $2 \times 2$  windows is simply a stride-2, depthwise,  $2 \times 2$  convolution with a weight set of four times  $1/4$ . Max. pooling has the same connectivity, just that the weights are 1 rather than  $1/\text{PoolingWindowSize}$ . Thus, only the neuron-update routine must change for max. pooling, not the proposed ESU-PEG pair.

**Dense Layers:** A fully-connected layer from  $N$  to  $N^+$  neurons is the same as a  $1 \times 1$  convolution between two FMs of shape  $N \times 1 \times 1$  and  $N^+ \times 1 \times 1$ , which is naturally supported. In this case, each neuron is an individual feature. Thus, all neurons in the destination population depend on all neurons in the source population.

**Flattening & Global Pooling:** Flattening an FM of shape  $D \times W \times H$  followed by a dense layer with  $N$  neurons (i.e., destination FM shape is  $N \times 1 \times 1$ ) is implemented as a single regular convolution with a kernel shape equal to the source FM width and height with  $N$  output channels. Thereby, the two layers are merged into one. Global pooling (average or max.) is realized in the same way, only that a depthwise connectivity has to be implemented.

**Nearest-Neighbor & Bilinear Interpolation:** An upsampling together with an interpolation, requires to combine the upsampling feature with an untrainable depthwise convolution representing the interpolation between the upsampled points.

**Add and Multiply Layers:** Add layers and pointwise multiply layers require two individual source FMs of the same shape pointing to the same destination FM. Between the two individual source FMs and the destination FM the same pointwise synaptic connectivity is required, implemented as the connectivity of a depthwise  $1 \times 1$  convolution with a single weight of 1 shared by both source FMs.

## 5 EXPERIMENTAL RESULTS

This section presents the experimental results. First, a silicon implementation for an event-based DNN accelerator is discussed. Subsequently, the compression gains for state-of-the-art CNNs are investigated.

### 5.1 Silicon Implementation

A variant of the PEG-ESU pair supporting all layer types is implemented in our next-generation *GrAI* architecture, taped-out in the TSMC12 FinFET technology with commercial availability projected for 2022. The heart of the 60 mm<sup>2</sup> SoC (shown in Fig. 1 on page 2) is a self-contained, event-based accelerator, supporting standard DNNs, LIF-NNs, and SD-NNs with over 18 million neurons.

The individual cores are arranged as an XY mesh connected through an NoC. By using an 8-bit relative core

address (4-bit  $X$ , 4-bit  $Y$ ), a neuron can have a synaptic connection with any neuron in the same core or any of the nearest 255 cores, while enabling the architecture to theoretically scale to an arbitrary number of cores. Our pre-product chip for embedded applications has 144 cores per die, but chip tiling—enabled by the relative addressing scheme—still allows for meshes with larger core counts.

Due to the self-contained nature, all neurons, weights, and other parameters mapped to a core have to fit into the on-chip SRAMs. Each core contains 256 kB of unified memory (with 64-bit words and 15-bit addresses) that can be allocated freely to weights, neuron states, and connectivity. To utilize the memory optimally, the architecture uses 8 bits to describe the width and height of a neuron population and 10 bits to describe the depth. This is enough for today's most popular CNNs. Larger populations can still be realized through FM cutting. The addressing allows a single population to fit over 1 million neurons. Still the descriptor of a neuron population containing width, height, depth, neuron type, activation function, axon count and start address of the population in the memory (axons and states are stored in a continuous block to avoid the need to fit two 15-bit addresses in the descriptor) fit in one 64-bit word.

Four bits are used to store the kernel width,  $KW$ , and height,  $KH$ , in the axons and kernel descriptors. The selection of the bit width used for kernel width and height are an important design choice. Together with the width of an  $XY$  coordinate (here 8 bit) they determine the width of most blocks in PEG and ESU data paths, as well as the maximum range of the *for loops* implemented through a state machine.

We found that rarely a CNN has a kernel size larger than 16. Hence, the used 4-bit does not only yield a low hardware complexity but also an efficient support of most CNNs. Note that, due to the flexibility provided by the offset fields,  $X_{\text{off}}$  and  $Y_{\text{off}}$ , any larger kernel can still be implemented through multiple axons and weight matrices (e.g., a  $32 \times 16$  convolution is realized as a  $16 \times 16$  convolution paired with another  $16 \times 16$  convolution between the same FMs for which the  $X_{\text{offset}}$  is increased by 16). For the upsample and stride fields 3 bit and 1 bit are used, respectively—enough for all common CNNs. Nevertheless, larger up- and downsample factors can be realized by adding dummy layers with an identity weight matrix.

With 8-bit  $XY$  coordinates and 4-bit kernel dimensions, 9 bits are enough for the signed  $X_{\text{off}}$  and  $Y_{\text{off}}$  values. We constrain FM fragments created by the mapper to have a width and height of at least 8 neurons (except for the last remaining cuts towards the left and bottom), which allows to reduce the bit width for  $W$  and  $H$  in the *axons* and the hardware complexity of the hit detection. This implies in practice no limitation, as the fragmentation by channels is not limited, which is strongly preferable anyway.

Given all that, also an axon and a kernel descriptor fit comfortably into a single 64-bit word. We made the design choice to have a kernel descriptor per channel of the source FM instead of only one per FM; i.e.,  $c_{\text{src}}$  of the event is used besides  $ID_p$  to select the kernel descriptor. A kernel descriptor contains the 3D kernel shape ( $KD, KW, KH$ ), and a pointer to the start address of the resulting 3D sub-weight-matrix,  $\mathbf{W}_{\text{sub}, c_{\text{src}}} = \mathbf{W}_{i,j,k,l|l=c_{\text{src}}}$ , in the memory. Moreover, the kernel descriptor contains information re-

quired for zero-weight skipping and weight quantization, which is not relevant for this work.

Multiple kernel descriptors per layer enable weight reuse among different source channels as well as different quantization and pruning schemes for each sub-weight-matrix. Also, it overcomes the need to calculate the start point in the weight matrix the descriptor points at. All weights in the sub-matrix are always used on an event processing. The drawback is a slightly reduced compression as we need at least  $C_{\text{src}}$  rather than 1 weight descriptor per layer.

Each neuron can have a persistent state for SD-NN or LIF-NN inference, or can dynamically allocate a temporary accumulator state for regular DNN implementations. Dynamic state allocation allows to map CNNs with larger neuron counts, as state entries can be shared among neurons whose accumulation phases are mutually exclusive. A state is a 16-bit float number for maximum precision, while a weight can be quantized to 8 bits or even less with no noticeable performance loss using adaptive float quantization [19].

Other than that, the architecture supports multi threading, single-instruction-multiple-data (SIMD) execution, as well as a wide range of neuron types and activation functions. Also, ESU and PEG still support absolute/non-compressed synapses for smaller networks with irregular connectivity.

### 5.1.1 Impact on Power, Performance, and Area

In the following, we summarize the results of the physical implementation in the 12-nm technology. The PEG and ESU take in total less than 2% of the area of a processor node. Only a marginal fraction ( $\ll 1\%$ ) of the power consumption is due to the ESU or the PEG, which are also not found to be part of the critical timing path. Note that the implemented ESU and PEG include many additional features beyond the scope of this paper. Examples are support for multi threading, weight quantization plus zero skipping, and non-compressed synaptic connectivity. Thus, the hardware costs of the proposed technique are negligible.

In line with previous work [11]—and despite applying the synapse compression—area, power, and timing of the chip are dominated by the on-chip memories used to store the weights and parameters. The memories take over 70% of the core area as shown in Fig. 1 on page 2. Thus, the power and area savings of the proposed technique are determined by the memory savings, investigated in the next subsection.

## 5.2 Compression Results

Through a Python tool, the memory gains of the proposed synapse-compression technique are quantified. The tool calculates the synaptic-memory requirements of a given CNN for the proposed method, the naive LUT approach, and the reference hierarchical-LUT approach [6], [8]. For the proposed technique, other than for the reference techniques, the memory requirements of a layer increases with the number of fragments the layer is split in. Thus, the tool calculates the memory requirements for the proposed scheme considering FM cuts that ensure that the total memory footprint of each resulting fragment is below 256 kB, which is the single core limit of our chip. By considering the real (non-beneficial) required FM cuts in the proposed technique, we report realistic rather than optimistic gains for the proposed technique.

To enable a detailed analysis, the memory requirements are categorized in *neurons*, *connectivity*, and *parameters*. The reported values for *connectivity* are the bits required to store the connectivity between the neurons, but they do not include the weights of the synaptic connections. Thus, for the proposed technique it includes axons, kernel descriptors, and population descriptors. Weights are included in the category *parameters*. The last section, *neurons*, is the memory allocated for neuron states. Throughout this section, we assume that a persistent 16-bit state is allocated for each neuron in a population. Reporting the memory usage in these categories allows to access the gains of pattern sharing and axon-based synapse computation in isolation. The former technique reduces the *parameter* requirements, while the latter reduces the *connectivity* requirements.

In the experiments, the tag width in the reference hierarchical-LUT technique is 15 bits. This is the minimum tag width required by the scheme to be able to map all CNNs analyzed in this work, as the analyzed networks have neurons with a fan-in (i.e., number of incoming synapses) as high as  $7^2 \cdot 512$ . Thereby, we present best-case values for the hierarchical-LUT reference technique, which in this form is not able to map any CNN with a considerably larger fan-in for any neuron. The unified memory can theoretically fit  $2^{17}$  16-bit neuron states in 256 kB of unified memory. Still, for the naive LUT technique, we consider 15-bit neuron addresses, as none of our experiments resulted in any core memory that is occupied more than 25 % by neurons for this technique. Hereby, we ensure a fair comparison also for the second reference technique.

By considering persistent 16-bit states for each neuron but 8-bit weights/parameters, we present conservative compression gains for the proposed technique, which heavily compresses the *parameters* and the *connectivity* compared to reference techniques, but not the *neurons*. Generally, both, the effectively required bits per neuron and per parameter, can be reduced further by compression techniques orthogonal to the one proposed in this work (e.g., non-persistent states, weight pruning, entropy coding, channel pruning) [11], [20]. However, reducing the two memory footprints also increases the compression gains of our technique substantially, as the heavily compressed connectivity in our scheme would have a higher impact in this case.

Through this experimental setup, we ensure that the reported gains of our technique are realistically achieved in practically all applications of event-based architectures. At the downside, the setup results in very pessimistic total memory requirements, why the reported values give no hint about the mapability of the analyzed CNNs. Thus, the **reported memory requirements are far above what is realistically achieved in our chip**, which also supports many parameter and neuron compression schemes orthogonal to the proposed technique.

### 5.2.1 Small CNNs

We start by analyzing a relatively small CNN for today's standards, *PilotNet* [10]. Its a 9-layer CNN used for autonomous driving. This example is discussed in-depth first, as it allows to understand the advantages as well as challenges revealed by the proposed technique. Also, *PilotNet* is the network that was demonstrated to fit in *Intel's* newest

event-based architecture, *Loihi 2*, making it a good reference benchmark. In the following subsection, we will validate the findings for other (much larger and advanced) networks.

We calculate the memory requirements of each layer for the proposed and the two reference techniques. The results are plotted in Fig. 6. They show that the memory requirements of the two other published techniques are dominated by *connectivity*. For the two techniques, LUT and hierarchical LUT, 74.1 %, and 65.2 % of the memory requirements are due to *connectivity*, respectively. The *parameters* are the second dominant factor for the memory requirements of reference techniques with a usage of about 25–35 %. As the weights are 8-bit quantized in this experiment, for non-quantized 16-bit weights, the *parameter* requirements will start to compete with the *connectivity* requirements.

Despite allocating a 16-bit state per neuron, the *neurons* only account for 0.2 %–0.3 % of the memory requirements for the reference techniques. This proves that synapse compression—as done by the proposed technique—is the most effective way to reduce the memory requirements for event-based architectures today.

The proposed synapse-computation methodology drastically reduces the *connectivity* and *parameter* requirements by a factor of  $15.6k \times$  and  $107 \times$ , compared to the best previously published method. *Intel* claims for the upcoming *Loihi 2* architecture a CNN synapse compression of up to  $17 \times$ .<sup>3</sup> The synapses, i.e., the combination of *parameters* and *connectivity*, are compressed by the proposed technique by a factor of  $305 \times$ , so an additional  $18 \times$  on top of the  $17 \times$  published recently by *Intel* [2].

*Connectivity*, from being the biggest contributor to the memory requirements, effectively becomes negligible with the proposed technique, contributing only 0.7 % to the memory usage. *Parameters*, on the other hand, are still dominant (53.7 %), despite the weight-sharing scheme. *Neurons* start to become an important factor (45.6 %) as well. However, this is only due to the persistent neuron states. Otherwise the memory requirements become dominated by weights, showing the high memory efficiency of our architecture supporting non-persistent states and weight compression through pruning and low bit-width adaptive float quantization.

Fig. 6 shows that with the proposed technique the memory requirements of the first layers are dominated by *neurons* (for the considered statefull neurons), while, for later layers, *parameters* take the largest share. This strongly justifies the need for an unified memory where the section sizes for *parameters* and *neurons* can be freely assigned, as done in our taped-out chip. The growing ratio of *neuron* over *parameter* requirements is explained with the structure of a typical CNN. Early layers have a larger XY resolution than later ones, as stride-2 convolutions, non-padded convolutions, and pooling layers successively reduce the width,  $W$ , and height,  $H$ , of the FMs. On the other hand, the channel count,  $D$  increases with the depth of the layer in most CNNs. Since the neuron and weight counts of a regular convolution layer are  $D \cdot W \cdot H$  and  $D_{src} \cdot D \cdot K \cdot W \cdot K \cdot H$ , respectively, weight

3. As of writing this paper, only maximum compression results are available for *Loihi 2* from [2]. The details of the used technique are not fully disclosed, why not more comparisons with *Loihi 2* can be drawn.

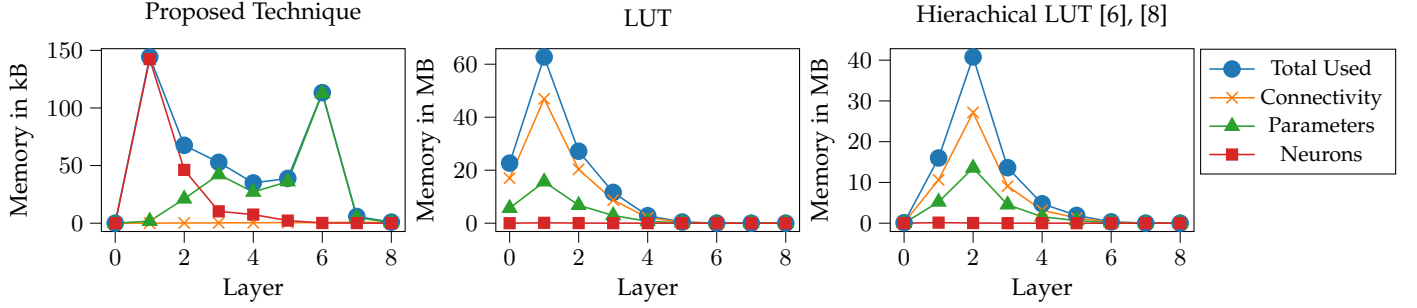


Fig. 6. Memory requirements for *PilotNet* [10] with the proposed and reference techniques mapping. Note the different Y scale (kB vs. MB).

requirements increase and neuron requirements decrease with the layer depth.

Most layers of the *PilotNet* CNN only take a small portion of the memory of a core (256 kB), despite analyzing a setup that has relatively high parameter and state requirements. Consequently, a mapping aiming at a minimized core count, showed that the proposed synapse-compression technique allows to fit the CNN without any further optimization in as few as 3 out of the 144 cores, as our architecture supports to map multiple layers to a core. With the two reference techniques the same mapping experiment shows a core count requirement that is at least  $101\times$  higher.

### 5.3 State-of-the-art CNNs

Existing event-based architectures do not support sophisticated CNNs. The reason is that such complex networks do not fit in the local memories due to the large synaptic memory requirements. The proposed technique overcomes this limitation through its large compression rates, as shown in the following.

We analyze the core and memory requirements for four of today's most popular CNNs: *Google's MobileNet* [9], *ResNet50* [1], *Darknet53* [21], and *ResNet101* [1]. The first network is designed to run on mobile devices and is thus more lightweight than the other three designed for less constrained devices such as GPUs. Hence, *MobileNet* has far fewer neurons and synapses than the other three analyzed CNNs (but still many more than *PilotNet*). In particular, *ResNet101* is an extremely complex network, while *ResNet50* and *Darknet53* are somewhere in the middle. We investigate these CNNs, to quantify the gains of the proposed technique for a broad range of network types. Also, we show that the proposed compression technique enables the execution of complex CNNs in a single self-contained chip.

The experimental setup here is the same as for the *PilotNet* analysis in the previous subsection.

Table 2 includes the results for all analyzed networks. The results show that with the previously published techniques, mapping CNNs more complex than *PilotNet* is out of reach, as for each network the memory requirements for *connectivity* is already far above the reasonable on-chip memory limit. This changes with the proposed technique, which compresses the memory footprint of *connectivity* compared to the best reference technique by up to  $15k\times$ . In fact, for all networks, the *connectivity* requirements become negligibly small. Even for the extremely complex *ResNet101* only about

TABLE 2  
Mapping of state-of-the-art CNNs with the proposed synapse-compression scheme versus prior art (in brackets the compression rates of the proposed scheme compared to prior art).

| CNN                   | Syn. Compr. | Mem. Total                  | Neurons                   | Connectivity                  | Parameters                  |
|-----------------------|-------------|-----------------------------|---------------------------|-------------------------------|-----------------------------|
| <i>PilotNet</i> [10]  | This Work   | 0.45 MB                     | 0.20 MB                   | 3.16 kB                       | 0.24 MB                     |
|                       | LUT         | 0.11 GB<br>(262 $\times$ )  | 0.20 MB<br>(1 $\times$ )  | 91.44 MB<br>(29.6k $\times$ ) | 25.63 MB<br>(107 $\times$ ) |
|                       | Hier. LUT   | 74.30 MB<br>(166 $\times$ ) | 0.20 MB<br>(1 $\times$ )  | 48.46 MB<br>(15.6k $\times$ ) | 25.63 MB<br>(107 $\times$ ) |
| <i>MobileNet</i> [9]  | This Work   | 11.23 MB                    | 8.00 MB                   | 0.16 MB                       | 3.07 MB                     |
|                       | LUT         | 1.85 GB<br>(169 $\times$ )  | 8.00 MB<br>(1 $\times$ )  | 1.38 GB<br>(8.9k $\times$ )   | 0.46 GB<br>(154 $\times$ )  |
|                       | Hier. LUT   | 1.34 GB<br>(123 $\times$ )  | 8.00 MB<br>(1 $\times$ )  | 0.88 GB<br>(5.7k $\times$ )   | 0.46 GB<br>(154 $\times$ )  |
| <i>ResNet50</i> [1]   | This Work   | 43.48 MB                    | 17.71 MB                  | 1.31 MB                       | 24.45 MB                    |
|                       | LUT         | 14.60 GB<br>(344 $\times$ ) | 17.71 MB<br>(1 $\times$ ) | 11.03 GB<br>(8.6k $\times$ )  | 3.54 GB<br>(149 $\times$ )  |
|                       | Hier. LUT   | 10.26 GB<br>(242 $\times$ ) | 17.71 MB<br>(1 $\times$ ) | 6.70 GB<br>(5.2k $\times$ )   | 3.54 GB<br>(149 $\times$ )  |
| <i>DarkNet53</i> [21] | This Work   | 51.21 MB                    | 21.19 MB                  | 1.36 MB                       | 28.66 MB                    |
|                       | LUT         | 25.13 GB<br>(502 $\times$ ) | 21.19 MB<br>(1 $\times$ ) | 18.63 GB<br>(14.0k $\times$ ) | 6.48 GB<br>(231 $\times$ )  |
|                       | Hier. LUT   | 18.68 GB<br>(374 $\times$ ) | 21.19 MB<br>(1 $\times$ ) | 12.18 GB<br>(9.2k $\times$ )  | 6.48 GB<br>(231 $\times$ )  |
| <i>ResNet101</i> [1]  | This Work   | 72.23 MB                    | 27.47 MB                  | 2.18 MB                       | 42.57 MB                    |
|                       | LUT         | 28.02 GB<br>(397 $\times$ ) | 27.47 MB<br>(1 $\times$ ) | 20.98 GB<br>(9.8k $\times$ )  | 7.01 GB<br>(169 $\times$ )  |
|                       | Hier. LUT   | 20.25 GB<br>(287 $\times$ ) | 27.47 MB<br>(1 $\times$ ) | 13.21 GB<br>(6.2k $\times$ )  | 7.01 GB<br>(169 $\times$ )  |

2 MB of memory, which is far below the on-chip memory limit of embedded architectures. Thus, in combination with the other supported compression techniques to bring the *parameter* and *neuron* requirements down by several times, even *ResNet101* is mappable in our architecture.

Due to the nature of the experimental setup, *parameters* and *neurons* dominate with the proposed synapse compression technique. Still, our weight sharing approach enables to bring the *parameter* requirements down by up to  $231\times$ .

Despite the conservative experiment, we achieve overall memory compression rates in the range from  $123\times$  to  $374\times$  compared to the published state of the art. A remarkable advantage of the proposed technique is that it has larger gains for complex networks. The memory compression rate for the lightweight CNNs, *MobileNet* and *Pilotnet*, are the lowest. For the complex CNNs *Darknet53* and *ResNet101* — for which a high compression rate is crucial—the overall compression is about  $300\times$ .

The reason is that in complex CNNs layers have many



more channels, resulting in many more synapses per neuron. With an increasing synapse-count per neuron, the compression rate of the proposed technique grows, as our technique only requires one axon to describe the connectivity between two neuron populations, irrespective of the synapse count in-between. This increases the mapability of complex CNNs on our event-based architecture.

Finally, we want to draw an abstract comparison with *Loihi 2*, for which the technology brief claims a synapse compression of up to  $17\times$  for CNNs without disclosing the technique fully [2]. Compared to the stated  $17\times$  best-case reduction by *Loihi2*, we achieve another factor of at least  $18\times$  (*PilotNet*) and up to  $37\times$  (*DarkNet53*) **on top**. This demonstrates the clear advantage of the proposed technique over not only the published state of the art but also upcoming commercial architectures.

## 6 CONCLUSION

This work presented a novel technique to compress the synaptic memory in neuromorphic event-based architectures running CNN benchmarks based on two novel lightweight hardware blocks substituting memory costly look-up tables. Our proposed technique has been taped-out in a 144-core event-based CNN accelerator using a 12-nm technology. The added hardware has negligible implementation costs. Nevertheless, it demonstrates compression rates for various modern CNNs ranging from  $123\times$  to  $374\times$ .

A systematic combination of the proposed technique with *orthogonal* weight and neuron compression schemes is left for future work. With such techniques we are even able to run extremely complex CNNs on our small form-factor *GrAI-VIP* chip in a temporal-sparse, event-based fashion at an ultra-low power consumption, latency, and cost.

## ACKNOWLEDGMENTS

This publication is supported by the *EU Horizon 2020* project, *ANDANTE*, which has received funding from the *ECSEL Joint Undertaking* (JU) under grant agreement No. 876925.

## REFERENCES

- [1] K. He, X. Zhang, S. Ren, and J. Sun, "Deep residual learning for image recognition," in *Proceedings of the IEEE conference on computer vision and pattern recognition*, 2016, pp. 770–778.
- [2] "Taking neuromorphic computing with *Loihi 2* to the next level – Technology Brief," <https://download.intel.com/newsroom/2021/new-technologies/neuromorphic-computing-loihi-2-brief.pdf>, (Accessed on 10/21/2021).
- [3] O. Moreira, A. Yousefzadeh, F. Chersi, A. Kapoor, R.-J. Zwartenkot, P. Qiao, G. Cinserin, M. A. Khoei, M. Lindwer, and J. Tapson, "Neuronflow: A hybrid neuromorphic–dataflow processor architecture for AI workloads," in *2020 2nd IEEE International Conference on Artificial Intelligence Circuits and Systems (AICAS)*. IEEE, 2020, pp. 01–05.
- [4] F. Akopyan, J. Sawada, A. Cassidy, R. Alvarez-Icaza, J. Arthur, P. Merolla, N. Imam, Y. Nakamura, P. Datta, G.-J. Nam *et al.*, "Truenorth: Design and tool flow of a 65mW 1 million neuron programmable neurosynaptic chip," *IEEE transactions on computer-aided design of integrated circuits and systems*, vol. 34, no. 10, pp. 1537–1557, 2015.
- [5] P. O'Connor and M. Welling, "Sigma delta quantized networks," *arXiv preprint arXiv:1611.02024*, 2016.
- [6] S. Moradi, N. Qiao, F. Stefanini, and G. Indiveri, "A scalable multicore architecture with heterogeneous memory structures for dynamic neuromorphic asynchronous processors (DYNAPs)," *IEEE transactions on biomedical circuits and systems*, vol. 12, no. 1, pp. 106–122, 2017.
- [7] S. B. Furber, F. Galluppi, S. Temple, and L. A. Plana, "The spinaker project," *Proceedings of the IEEE*, vol. 102, no. 5, pp. 652–665, 2014.
- [8] M. Davies, N. Srinivasa, T.-H. Lin, G. Chinya, Y. Cao, S. H. Choday, G. Dimou, P. Joshi, N. Imam, S. Jain *et al.*, "Loihi: A neuromorphic manycore processor with on-chip learning," *IEEE Micro*, vol. 38, no. 1, pp. 82–99, 2018.
- [9] A. G. Howard, M. Zhu, B. Chen, D. Kalenichenko, W. Wang, T. Weyand, M. Andreetto, and H. Adam, "MobileNets: Efficient convolutional neural networks for mobile vision applications," *arXiv preprint arXiv:1704.04861*, 2017.
- [10] M. Bojarski, D. Del Testa, D. Dworakowski, B. Firner, B. Flepp, P. Goyal, L. D. Jackel, M. Monfort, U. Muller, J. Zhang *et al.*, "End to end learning for self-driving cars," *arXiv preprint arXiv:1604.07316*, 2016.
- [11] S. Han, H. Mao, and W. J. Dally, "Deep compression: Compressing deep neural networks with pruning, trained quantization and Huffman coding," *arXiv preprint arXiv:1510.00149*, 2015.
- [12] S. Xie, R. Girshick, P. Dollár, Z. Tu, and K. He, "Aggregated residual transformations for deep neural networks," in *Proceedings of the IEEE conference on computer vision and pattern recognition*, 2017, pp. 1492–1500.
- [13] B. Jacob, S. Kligys, B. Chen, M. Zhu, M. Tang, A. Howard, H. Adam, and D. Kalenichenko, "Quantization and training of neural networks for efficient integer-arithmetic-only inference," in *Proceedings of the IEEE conference on computer vision and pattern recognition*, 2018, pp. 2704–2713.
- [14] M. Rastegari, V. Ordonez, J. Redmon, and A. Farhadi, "XNOR-net: ImageNet classification using binary convolutional neural networks," in *European conference on computer vision*. Springer, 2016, pp. 525–542.
- [15] T. Serrano-Gotarredona, B. Linares-Barranco, F. Galluppi, L. Plana, and S. Furber, "ConvNets experiments on SpiNNaker," in *2015 IEEE International Symposium on Circuits and Systems (ISCAS)*. IEEE, 2015, pp. 2405–2408.
- [16] A. Zhang, Z. C. Lipton, M. Li, and A. J. Smola, "Dive into deep learning," *arXiv preprint arXiv:2106.11342*, 2021.
- [17] Y. Cao, Y. Chen, and D. Khosla, "Spiking deep convolutional neural networks for energy-efficient object recognition," *International Journal of Computer Vision*, vol. 113, no. 1, pp. 54–66, 2015.
- [18] O. Ronneberger, P. Fischer, and T. Brox, "U-net: Convolutional networks for biomedical image segmentation," in *International Conference on Medical image computing and computer-assisted intervention*. Springer, 2015, pp. 234–241.
- [19] T. Tambe, E.-Y. Yang, Z. Wan, Y. Deng, V. J. Reddi, A. Rush, D. Brooks, and G.-Y. Wei, "Adaptivefloat: A floating-point based data type for resilient deep learning inference," *arXiv preprint arXiv:1909.13271*, 2019.
- [20] Y. He, X. Zhang, and J. Sun, "Channel pruning for accelerating very deep neural networks," in *Proceedings of the IEEE international conference on computer vision*, 2017, pp. 1389–1397.
- [21] J. Redmon and A. Farhadi, "Yolov3: An incremental improvement," *arXiv preprint arXiv:1804.02767*, 2018.